Joint Optimization of Semi-Passive IRS Phase Shifts and NOMA Power Coefficients for Cooperative CRNs

Joint Optimization of Semi-Passive IRS Phase Shifts and NOMA Power Coefficients for Cooperative CRNs

***Abstract*—In this study, we investigate the incorporation of an intelligent reflecting surface (IRS) into cooperative spectrum-sharing cognitive radio networks (CRNs). Specifically, we investigate a strategy for sharing spectrum between the primary and secondary networks, consisting of a primary user (PU) and multiple secondary users (SUs). The data transmission process is split into two phases. In the first phase, the primary transmitter is assisted by an IRS (which is controlled by the secondary transmitter (ST)) to serve the PU. This arrangement allows the primary network to allocate a part of its spectrum to the users within the secondary network. In the subsequent phase, the ST employs a non-orthogonal multiple access (NOMA) transmission technique to simultaneously serve the PU and SUs. By utilizing a semi-passive IRS, both data transmission to the PU and channel estimation of SUs are performed simultaneously during the first transmission phase. The core objective is to improve the weighted sum-rate of the CRN through a joint optimization of the NOMA power coefficients and IRS phase adjustments during the second transmission phase. We propose an effective algorithm that breaks down the primary sum-rate maximization problem into two sub-problems. The IRS phase shifts are computed, followed by the optimization of the NOMA power coefficients. These coefficients are iteratively refined until a convergence is reached. Through simulations, we demonstrate that the proposed algorithm yields substantial gains in the sum-rate performance compared to existing methods.**

***Index Terms*—Intelligent reflecting surface, cognitive radio networks, power allocation, non-orthogonal multiple access, weighted sum-rate.**

I. Introduction

THE deployment of 5G communication systems is currently underway in many regions around the world. The 5G network fulfills the current traffic demand by employing various effective technologies [1]. However, it may not be able to keep up with the future applications expected by 2030 [2] such as holographic-type communication, autonomous vehicles, virtual reality, tactile internet, etc. [3], [4]. In addition to this, these applications will also require high bandwidth, low latency and robust security. Therefore, the research interest towards the future communication network i.e., 6G, has seen significant rise recently. As of now, many promising enabling technologies have been identified for 6G systems capable of meeting rigorous requirements of future applications. Some of the promising 6G enabling technologies include terahertz (THz) communications, artificial intelligence (AI), quantum computing, visible-light communications (VLC) and intelligent reflecting surfaces (IRSs) [3].

Since 5G networks operate in the millimeter wave (mmWave) range of the spectrum, high directivity causes mmWave communication signals to be prone to blockages, especially in indoor communications. Consequently, to enhance the efficacy of wireless networks, the concept of a reconfigurable wireless channel environment has emerged recently. Within this context, the Intelligent Reflecting Surface (IRS) emerges as a promising technology, capable of overcoming blockage challenges to establish uninterrupted wireless links for mmWave and THz networks [5]. Furthermore, the IRS technology has been shown to be capable to enhance network performance in aspects such as spectrum utilization and energy efficiency [6].

An IRS is a two-dimensional (2D) planner metasurface which consists of a large number of reflecting elements (such as low-cost printed antennas), which can reflect the incident signal passively [7], hence providing a programmable propagation environment [6]. An IRS is a three-layer device that is connected to a smart controller. Numerous metallic sections are etched onto a dielectric substrate within the outermost layer, facilitating immediate engagement with incoming signals. Adjacent to this layer, a copper plate is positioned to hinder any dissipation of the signal's energy. The innermost layer comprises a control circuit board which helps in adjusting the amplitude and phase shift of each discrete component. This adjustment process is activated through a microcontroller linked to the IRS. This microcontroller is a gateway to communicate with other network infrastructures, such as base stations (BSs) and access points (APs). Specifically, a separate low-rate link exists between the IRS and the controlling devices for the information exchange [8]. IRS technology can be implemented for coverage extension and interference avoidance. IRS can also be deployed to improve security [9] and support simultaneous wireless information and power transfer [10].

The IRS offers numerous benefits when put into practice. To begin with, unlike standard active antenna arrays or surfaces [11], the IRS does not require transmitting radio-frequency (RF) chains, making the IRS an energy-efficient technology [12]. An IRS operates in the full-duplex mode, but does not experience self-interference as full-duplexing does not amplify antenna noise or experience self-interference. These features give it a competitive advantage over those active relay technologies, such as the half-duplex and FD relay. Moreover,

M. Khan, J. Mirza and B. Ali are with the Department of Electrical and Computer Engineering, COMSATS University Islamabad, Islamabad 45550, Pakistan (Emails: mhsnkhaan@gmail.com, jaydee.mirza@gmail.com, bakhtiar_ali@comsats.edu.pk).

an IRS is also simple to deploy and can be embedded on other objects in the environment because of its lightweight and conformal geometry [13]. Inspired by these exceptional features, studies have shown that the performance of the network improves by effectively designing the reflection coefficients of the IRS [14]–[17].

Due to the attractive features of IRS technology, its impact on the performance of the network has been evaluated by integrating it with other existing technologies. For instance, IRS has been combined with non-orthogonal multiple access (NOMA)-based communication systems [18]–[22]. These studies report that the performance of such integrated systems are superior to conventional NOMA systems without IRS, in terms of received signal strength [18], less transmission power [19], outage probability [20] and data rates [21]. In addition to NOMA systems, IRS-aided cognitive radio networks (CRNs) have also been investigated in the literature. Existing studies have reported the benefits obtained by deploying the IRS in CRNs [23]–[25], in terms of spectral and energy efficiency. As our proposed work considers an IRS-aided NOMA-based cooperative spectrum-sharing CRN, we present a brief overview of the related studies investigating the integration of these three important technologies.

A. Related Work

Spectrum efficiency and user connectivity can be enhanced up to a larger extent by deploying an IRS in a NOMA based CRN [26]. In the existing literature, few studies have investigated the performance gain offered by combining IRS, NOMA and cognitive radio technologies. In [26], a multiple-input single-output (MISO) CRN with NOMA was considered, which is aided by a single IRS. The main objective is to enhance spectral efficiency and energy efficiency of the network. To achieve this objective, the active beamforming vectors at the secondary transmitter (ST) and reflection coefficients (or phase shifts) of the IRS are optimized. It was reported that IRS assisted NOMA-based CRNs outperform NOMA-based CRNs without IRS, in terms of spectral efficiency. The improvement is due to the improved strength of received signals at secondary users (SUs) and effective interference mitigation. In [27], a NOMA-based CRN supported by the IRS was investigated in the presence of a primary user (PU), an ST serving multiple SUs and an eavesdropper. This investigation formulates analytical formulations to characterize the secrecy outage behavior of SUs aided by the IRS. The outcomes illustrate that increasing the number of reflective components within the IRS reduces the secrecy outage of the SU.

Authors in [28] conducted a study on the integration of an IRS into a NOMA-based underlay CRN which consists of a primary transmitter (PT), a PU, and an ST serving multiple SUs. The main idea of [28] is to enhance the energy efficiency of the network by jointly optimizing the beamforming vectors at the ST and IRS phase shifts. For this purpose, a second-order cone programming was used for active beamforming design, while the passive beamforming vector (phase shifts) was designed by applying a semidefinite relaxation (SDR) approach. It has been reported in [28] that the energy efficiency of the system improves as the number of reflecting elements in the IRS grows. Similarly, in [29], an IRS-assisted NOMA-based underlay CRN was investigated. The network is composed of a PT, a PU and an ST serving multiple SUs. A specific number of reflecting elements in the IRS are assigned to each SU. The investigation revealed that the IRS-assisted NOMA-based underlay CRN provides a 6 dB gain (with 2 SUs and an assignment of 16 reflecting elements per user) compared to the orthogonal multiple access (OMA) scheme without IRS. The studies in [26]–[29], demonstrated that the integration of IRS in NOMA-based CRNs ensures the PU quality of service (QoS) while appropriately designing the IRS phase shifts to assist SUs. As a result, the strength of received signals at the SUs is boosted, thus enhancing the spectral efficiency of the network.

The aforementioned studies are performed on IRS-aided NOMA-based underlay CRNs. In underlay CRNs, there is a constraint on the transmission power of the ST which limits the performance of SUs. Furthermore, IRS phase shifts need to be designed in such a way that the interference level at the PU is kept below a specific threshold. Moreover, the assistance of IRS to both primary and secondary networks has not been investigated. In the context of CRNs, the use of IRS-enabled joint data transmission and uplink channel estimation (CE) has not been investigated in the existing literature.

B. Our Contributions

Hence, motivated by [30], our work investigates the incorporation of the IRS within the cooperative spectrum-sharing CRN using NOMA principles. The system configuration includes a primary network comprising a PT and a PU, alongside a secondary network involving a ST and multiple SUs. The conceptual framework of this NOMA-based cooperative spectrum-sharing CRN consists of two distinct transmission phases. In our devised approach, the utilization of the IRS during the initial transmission phase facilitates the PU in fulfilling its data rate requisites. Capitalizing on this outcome, the PU subsequently grants SUs the opportunity to communicate to SUs using its spectrum during the subsequent transmission phase. Within this latter phase, the ST concurrently caters to the needs of both the PU and SUs using the NOMA principles, while ensuring that the PU's minimum rate prerequisites are met. A semi-passive IRS is utilized to simultaneously perform downlink data transmission to the PU and CE of SUs. The passive IRS elements reflect the incident signal from the PT to the PU, while in the same time the active elements of the IRS are tasked with receiving the uplink SU signal for the purpose of localization and CE of SUs. Given that the IRS is connected with the ST through a wired link (a common assumption made in the IRS literature), the estimated channel samples are sent to ST for the computation of channel parameters such as complex gain of each path along with associated angle of arrival (AoA) and angle of departure (AoD). Note that these channel parameters are not only useful for CE but also for the localization of SUs.

For the second transmission phase, we formulate a weighted sum-rate maximization problem where the reflection coefficients of the IRS are optimized along with NOMA power

coefficients at the ST. The formulated problem is a non-convex problem due to coupled optimization variables. To solve the non-convex optimization problem, we develop an efficient method in which the reflection coefficients of the IRS are optimized first by fixing the NOMA power coefficients. Then the NOMA power coefficients are optimized in an iterative manner, such that after each successful iteration the input rate vector to the algorithm is modified in small increments. The contributions of the paper are summarized below.

- Design of an IRS-assisted NOMA-based spectrum-sharing CRN to enhance the performance of the CRN. In the first transmission phase, the PU is served to by the PT. In the second phase, the ST efficiently serves both the PU and SUs through the PU-assigned spectrum. This cooperative spectrum-sharing paradigm proves mutually beneficial for both primary and secondary networks, significantly enhancing spectrum efficiency. Using semi-passive IRS, during the first transmission phase, passive IRS elements assist the data transmission of the primary network and active IRS elements are used for the CE of SUs.
- Formulation of an optimization problem pertaining to the second transmission phase. The primary objective of the considered optimization problem is to maximize the network's weighted sum-rate. The optimization task entails the joint optimization of the IRS's reflection coefficients and the NOMA power coefficients at the ST. To address this complex problem, a two-step approach is adopted. The first subproblem revolves around optimizing the IRS's reflection coefficients, addressed through the SDR technique. The second subproblem focuses on determining the NOMA power coefficients at the ST, accomplished with the closed-form expressions.
- Development of an efficient algorithm characterized by a low computational complexity. The algorithm aims to solve the problem of maximizing the weighted sum-rate. The algorithm's efficiency is enhanced by simplifying the first subproblem which involves optimizing the IRS reflection coefficients. Our analysis of the problem reveals that these coefficients need to be computed only once while keeping the NOMA power coefficients constant. Consequently, this strategy significantly reduces the overall complexity of the algorithm.

The rest of the paper is organized as follows. In Section II, signal and channel models are introduced. Section III presents the weighted sum-rate maximization problem and the proposed algorithm to solve the formulated problem. Moreover, numerical results are discussed in section IV to verify the effectiveness of the proposed algorithm. Finally, in section V, we conclude the paper.

Notations: In this paper scalar variables are denoted by lowercase letters while vectors and matrices are denoted by boldface lowercase and boldface uppercase, respectively. $\mathbb{C}^{M\times N}$ represents a complex-valued matrix of $M \times M$ size. The notation diag($\mathbf{x}$) represents diagonal operation on the elements of an arbitrary vector $\mathbf{x}$. Similarly, $\mathbf{x}^*$ and $\mathbf{x}^H$ represents conjugate and conjugate transpose of a vector $\mathbf{x}$, respectively. The symbol $\otimes$ is used to represent the Kronecker product. The rank and the trace of matrix $\mathbf{X}$ are symbolized by rank ($\mathbf{X}$) and Tr ($\mathbf{X}$), whereas $\mathbf{X} \succeq 0$ denotes that $\mathbf{X}$ is a positive semidefinite matrix.

II. System model

A. Signal model

We consider an IRS-assisted downlink NOMA-based cooperative spectrum-sharing CRN consisting of primary and secondary nodes as shown in Fig. 1. The primary nodes comprise of a PT that serves a single PU in the network. On the other hand, the secondary nodes consist of an ST that serves the PU and multiple SUs. There are total K number of users in the network, i.e., a single PU and $K-1$ SUs. It is assumed that each node is equipped with a single antenna. The proposed cooperative spectrum-sharing CRN system consists of two transmission phases as depicted in Fig. 2. An IRS is deployed in the surrounding area to assist the communication between the nodes. The IRS is equipped with a large number of low-cost reflecting elements. We consider a semi-passive IRS which employs both passive and active elements. We denote the total number of reflecting elements in the IRS by N. The total number of passive elements in the IRS is denoted by M and the total number of active elements is $N-M$, where it is assumed that $M > N-M$. The purpose of the active IRS elements is to perform uplink CE of SUs during the first transmission phase. We assume that the CE of the PU (both incident and reflected channels) is performed prior to the first transmission stage as shown in Fig. 2. We assume that the direct links are severely blocked by obstructions, whereas only the direct link between the PT and ST is reliable for communication. The IRS assists the PT and ST to establish communication with the users.

The IRS deployed in the network is connected to the ST through a wired connection which enables it to adjust the phase shifts of the IRS elements with the help of a microcontroller embedded on the IRS. In the first transmission phase, the ST permits the PT to communicate with the PU through the IRS, such that the ST adjusts the IRS phase shifts according to the reflective channels of the PT-PU link. In turn, the PT allows the ST to use the spectrum assigned to the primary network in the second transmission phase. The ST simultaneously serves the PU and SUs by using the spectrum shared by the primary network. As a result, both primary and secondary networks cooperate with each other for reliable communication.

As both downlink data transmission for the primary network and uplink CE for the secondary network are carried out simultaneously during the first transmission phase (see Fig. 1 and Fig. 2). Here, we assume that the PU is not affected by the interference from uplink pilot signals of the SUs. It is important to note that for both the transmission phases, only passive IRS elements are used to assist the communication. With the channel estimation errors, the phase shift matrix in the first and second transmission phases undergoes errors. These errors in the phase shifts affect the passive beamforming, resulting in performance degradation. In this study, we do not consider hardware impairments of the IRS and also assume

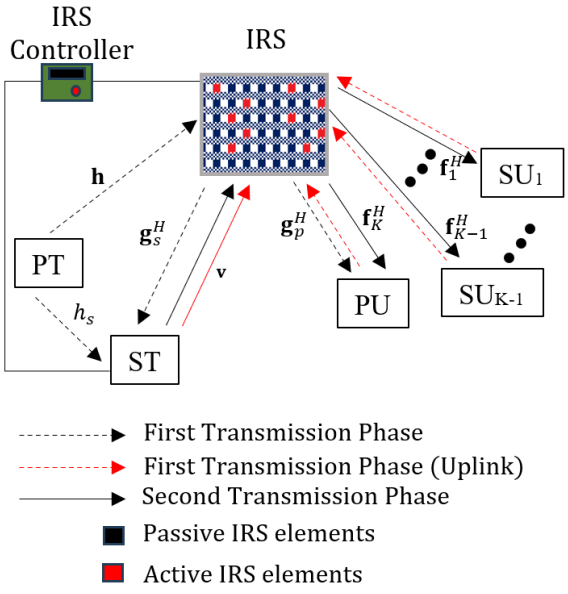

Fig. 1: An IRS assisted NOMA-based cooperative spectrum-sharing network where the PU is depicted as the K^{th} user in the second transmission slot with $\mathbf{g}_p^H = \mathbf{f}_K^H$.

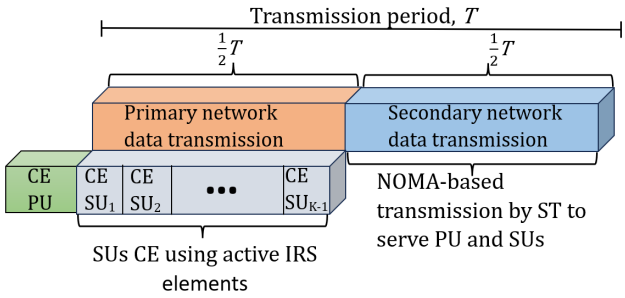

Fig. 2: An illustration of two transmission phases for the CRN with IRS.

perfect suppression of interference from the passive elements to the active elements of the IRS. The total transmission period is represented by T, which is equally divided between the primary and secondary networks as shown in Fig. 2. Now, we describe the signal model associated with the two transmission phases.

First Transmission Phase: The PT transmits the symbol x_p designated for the PU during the first transmission phase. This symbol is also received by the ST and SUs. The received signal at the PU in the first transmission phase is given by[1]

$$y_p^{(1)} = \sqrt{P_p}\left(\mathbf{g}_p^H \mathbf{\Theta}^{(1)} \mathbf{h}\right) x_p + n_p^{(1)}, \tag{1}$$

where P_p is the transmit power at the PT, $\mathbf{h} \in \mathbb{C}^{M\times 1}$ is the incident channel from the PT to the IRS and $\mathbf{g}_p \in \mathbb{C}^{M\times 1}$ is the reflected channel from the IRS to the PU. The diagonal phase shift matrix of the IRS in the first transmission phase is represented by $\mathbf{\Theta}^{(1)}$, such that $\mathbf{\Theta}^{(1)} = \text{diag}\left(\beta_1^{(1)} e^{j\theta_1^{(1)}}, \ldots, \beta_M^{(1)} e^{j\theta_M^{(1)}}\right)$. Here $\theta_m \in [0, 2\pi)$ and $\beta_m \in [0, 1)$ denote the phase and ON/OFF value of the reflection coefficient associative with the m^{th} reflecting element, respectively. $n_p^{(1)}$ is the additive white Gaussian noise (AWGN) at the PU with the zero mean and its variance equal to $\sigma_p^{2(1)}$.

Similarly, the signal received at the ST during the first transmission phase can be expressed as

$$y_s^{(1)} = \sqrt{P_p}\left(\mathbf{g}_s^H \mathbf{\Theta}^{(1)} \mathbf{h} + h_s\right) x_p + n_s^{(1)}, \tag{2}$$

where $\mathbf{g}_s \in \mathbb{C}^{M\times 1}$ is the reflected channel from the IRS to the ST and h_s is the direct channel from the PT to the ST. $n_s^{(1)}$ is the AWGN term at the ST having the zero mean and the variance equal to σ_s^2. In the first transmission phase, the desired user is the PU, which means that the phase shifts of the IRS need to be configured for improving the gain of the PT-PU. The achievable rate for the PU can be written as,

$$R_p^{(1)} = \frac{1}{2}\log_2\left(1 + \frac{P_p |\mathbf{g}_p^H \mathbf{\Theta}^{(1)} \mathbf{h}|^2}{\sigma_p^{2(1)}}\right). \tag{3}$$

Denoting the estimated channels of $\mathbf{h}$ and $\mathbf{g}_p$ by $\bar{\mathbf{h}}$ and $\bar{\mathbf{g}_p}$, respectively, we set the reflection coefficient of the m^{th} element as [31], $\angle\theta_m^{(1)} = -\angle\bar{h}_m^{(1)}\bar{g}_{p,m}^*$, where $\bar{h}_m^{(1)}$ is the incident channel from the PT to the m^{th} element of the IRS and $\bar{g}_{p,m}$ is the reflected channel at the PU from the m^{th} element of the IRS. Now, by setting $\beta_i^{(1)} = 1$, $i = 1, \ldots, M$, the phase shift matrix can be written as $\mathbf{\Theta}^{(1)} = \text{diag}\left(e^{j\angle\theta_1^{(1)}}, e^{j\angle\theta_2^{(1)}}, \ldots, e^{j\angle\theta_M^{(1)}}\right)$.

The uplink CE of the SUs can be performed along with the downlink data transmission of the primary network as shown in Fig. 2. For this purpose, SUs can utilize the first transmission phase by sending uplink pilot signals to the IRS elements in a TDMA manner. The active elements of the IRS are used to receive the pilot signals and perform CE, while the passive IRS elements are only used for downlink data transmission to PU.

Second Transmission Phase: The transmission of the PU symbol x_p in the first phase is followed immediately by the transmission of SUs messages in the second transmission phase. Since a cooperative spectrum-sharing CRN is considered in this paper, the ST will not only transmit SUs messages but it will also relay the PU symbol that was detected by the ST in the first transmission phase. The transmission of all the messages by the ST is realized by implementing the superposition coding (SC) principle of NOMA at the ST. According to SC, a superposed signal $\sum_{k=1}^{K}\sqrt{\alpha_k P_{st}}\, x_k$ is transmitted by the ST in the second transmission phase. P_{st} is the total transmission power at the ST, x_k is the symbol for the k^{th} user and a_k is the NOMA power allocation coefficient for the k^{th} user, such that $\alpha_k \in (0, 1)$. The superposed signal transmitted by the ST is received by all the K users (i.e., PU and SUs). Let $a_k = \alpha_k P_{st}$, and the signal received at the k^{th}

[1]The PU transmission is supported by the IRS, which significantly enhances the received signal strength at the PU, therefore, we assume that the interference level from the uplink SU transmission is comparatively small and thus can be ignored.

user in the second transmission phase is given by

$$y_k^{(2)} = \left(\mathbf{f}_k^H \mathbf{\Theta}^{(2)} \mathbf{v}\right) \sum_{k=1}^{K} \sqrt{a_k}\, x_k \; + n_k^{(2)}, \tag{4}$$

In the above equation, $\mathbf{f}_k \in \mathbb{C}^{M\times 1}$ is the reflected channel vector from the IRS to the k^{th} user and $\mathbf{v} \in \mathbb{C}^{M\times 1}$ is the incident channel vector from the ST to the IRS. In the second transmission phase, $\mathbf{\Theta}^{(2)} = \text{diag}(e^{j\theta_1^{(2)}}, \ldots, e^{j\theta_M^{(2)}}) \in \mathbb{C}^{M\times M}$ is a diagonal phase shift matrix of the IRS, and $n_k^{(2)} \sim \mathcal{CN}(0, \sigma_k^{2(2)})$ represents the AWGN at the k^{th} user.

The cascaded channel gain in the IRS-aided communication systems is determined not only by the incoming and outgoing channel gains of the IRS, but also by the phase shift matrix. Thus, in this study, we optimize the phase shift matrix $\mathbf{\Theta}^{(2)}$, to improve communication links of the ST with the PU and SUs. The optimization of the phase shift matrix $\mathbf{\Theta}^{(2)}$ is presented in Section III.

As we deploy the NOMA scheme in the second transmission phase, each user employs a successive interference cancellation (SIC) technique to remove other user symbols and extract its desired symbol from the superposed signal. For this purpose, users must be arranged in a specific decoding order. Therefore, the arrangement of the users in this work is based on the distance of the users from the IRS such that $d_1 \geq \cdots \geq d_k \geq \cdots d_K$. According to the NOMA decoding principle, the user $k = 1$ has the weakest channel gain and will directly decode its own signal by treating the signal of all the other users as interference. Similarly, for any k^{th} user, $k > 1$, the user will first decode the symbol of the l user, where $l < k$. This process continues until the symbols of all the l users are decoded and these symbols are removed from the received signal. While the symbols of users, $K-k$, will be considered as interference. In the same way, the K^{th} user will decode and remove the symbol of all users iteratively until its own symbol is decoded. Note that in our study, the K^{th} user is the PU, which is assumed to be the closest user from the IRS. Thus, the achievable rate of the k^{th} user, $k \neq K$, is given by

$$R_k^{(2)} = \frac{1}{2} w_k \log_2 \left(1 + \frac{|\mathbf{f}_k^H \mathbf{\Theta}^{(2)} \mathbf{v}|^2\, a_k}{|\mathbf{f}_k^H \mathbf{\Theta}^{(2)} \mathbf{v}|^2 \sum_{i=k+1}^{K} a_i + \sigma_k^{2(2)}}\right), \tag{5}$$

where, w_k is the non-negative weight factor assigned to k^{th} user, such that the weight vector is given by $\mathbf{w} = [w_1, w_2, \ldots, w_K]^T$. Similarly, the achievable data rate of the user K (i.e., PU) can be obtained by using

$$R_K^{(2)} = \frac{1}{2} w_K \log_2 \left(1 + \frac{|\ \mathbf{f}_K^H \mathbf{\Theta}^{(2)} \mathbf{v}|^2\ a_K}{\sigma_K^{2(2)}}\right). \tag{6}$$

Since, x_p is received at the PU in the first transmission phase, thus the overall achievable rate of the PU according to the decoding order, can be expressed as

$$R_p = R_p^{(1)} + R_K^{(2)}. \tag{7}$$

From this point onward, for the ease of notation, we assume an equal noise power at all the receivers and denote it with σ^2, such that $\sigma^2 = \sigma_p^{2(1)} = \sigma_s^{2(1)} = \sigma_k^{2(2)} = \sigma_K^{2(2)}$.

B. Channel model

We assume a narrowband 3-D geometric mmWave channel model for all the incident and reflected channels [32]. Denoting N_p as the total number of propagation paths, the channel between the PT and IRS can be written as

$$\mathbf{h} = \sum_{l=1}^{N_p} \alpha_l^h\ \mathbf{a}(\phi_l^{\text{AoA}}, \varphi_l^{\text{AoA}}), \tag{8}$$

where α_l^h represents the complex channel gain of the l^{th} path. The elevation angle of arrival (AoA) and azimuth AoA of the l^{th} path are denoted by ϕ^{AoA} and φ^{AoA}, respectively. The array response vector for any arbitrary values of elevation angle, ϕ, and azimuth angle, φ, can be written as [33]

$$\begin{aligned}\mathbf{a}(\phi, \varphi) =& [1, e^{j2\pi \frac{\lambda}{d_{\text{IRS}}} \cos\phi}, \ldots, e^{j2\pi(M_h-1)\frac{\lambda}{d_{\text{IRS}}}\cos\phi}]^T \\ &\otimes [1, e^{j2\pi \frac{\lambda}{d_{\text{IRS}}} \sin\phi \sin\varphi}, \ldots, \\ &\qquad e^{j2\pi(M_v-1)\frac{\lambda}{d_{\text{IRS}}}\sin\phi\sin\varphi}]^T, \end{aligned} \tag{9}$$

The inter-element distance of the IRS is denoted by d_{IRS} and λ is the wavelength. The quantities M_h and M_v represent the total number of reflecting elements along horizontal axis and vertical axis of the IRS, respectively. In the first transmission phase, the channel between the IRS and PU is expressed as

$$\mathbf{g}_p = \sum_{l=1}^{N_p} \alpha_l^g\ \mathbf{a}(\phi_l^{\text{AoD}}, \varphi_l^{\text{AoD}}), \tag{10}$$

where ϕ^{AoD} and φ^{AoD} denote the elevation angle of departure (AoD) and azimuth AoD of the l^{th} path. α_l^g represents the complex channel gain of the l^{th} path. The array response vector of the channel from the IRS to the PU is modelled using (9).

In the second transmission phase, the incident channel from the ST to the IRS and all the reflected channels including the channel from the IRS to the PU and SUs are modelled according to the narrowband 3-D geometric mmWave channel. Thus, the channel between the ST and IRS is given by $\mathbf{v} = \sum_{l=1}^{N_p} \alpha_l^v\ \mathbf{a}(\phi_l^{\text{AoA}}, \varphi_l^{\text{AoA}})$, where α_l^v represents the complex channel gain of the l^{th} path. Similarly, the reflected channel from the IRS to the k^{th} user can be written as $\mathbf{f}_k = \sum_{l=1}^{N_p} \alpha_l^{f_k}\ \mathbf{a}(\phi_l^{\text{AoD}}, \varphi_l^{\text{AoD}})$, where $\alpha_l^{f_k}$ represents the complex channel gain of the l^{th} path.

C. Uplink Channel Estimation

Here, we present the details of the CE technique used in this study. Given the narrowband mmWave 3-D geometric channel model, discussed in the previous subsection, we employ the CE method presented in [34]. Therein, active elements in the IRS are used to obtain the noisy samples of the channel. These sample values are then used along with the array response vector codebook to reconstruct the complete channel using compressed sensing techniques. The CE at the IRS is carried out during the first transmission phase. This means data transmission to the PU and CE of SUs are performed simultaneously.

The uplink CE of both incident channel and reflected channel for the PT-IRS-PU link is carried out at the beginning before the data transmission of the primary network as shown

in Fig. 2. We explain the CE process for the uplink SUs channel i.e., the channel between the k^{th} user and IRS. As we consider time division duplex (TDD) transmission, the uplink and downlink channels between the IRS and the k^{th} SU are assumed to be same due to the perfect channel reciprocity. Denoting the number of active elements in the IRS as $\bar{M}$, we can write the sampled noisy channel vector of size $\bar{M} \times 1$ for the k^{th} SU as

$$\bar{\mathbf{f}}_k = \mathbf{\Lambda}\mathbf{f}_k + \mathbf{n}, \tag{11}$$

where $\mathbf{\Lambda}$ represents the selection matrix of size $\bar{M} \times M$. The selection matrix selects the entries of the channel corresponding to the active elements in the IRS. In particular, the selection matrix, $\mathbf{\Lambda}$, comprises of the rows of an $M \times M$ identity matrix corresponding to the active elements of the IRS. The noise vector at the IRS is given by $\mathbf{n} \sim \mathcal{CN}(\mathbf{0}, \sigma^2\mathbf{I})$.

To reconstruct the complete channel vector, we define an array response dictionary, $\mathbf{D}$, containing $\mathcal{D}$ number of columns, each representing the array response vector based on (9) with quantized azimuth and elevation angles, such that $\mathbf{D} \in \mathbb{C}^{M \times \mathcal{D}}$. Similar to [34], we also assume that due to the high resolution of the dictionary, all N_p paths match with the different N_p columns of the the dictionary. Now, we can represent the channel, $\mathbf{f}_k$ as $\mathbf{f}_k = \mathbf{D}\mathbf{s}_k$, where $\mathbf{s}_k$ is the sparse vector of size $\mathcal{D} \times 1$ with non-zero entries equal to N_p. We can express the sampled noisy channel vector in (11) as

$$\begin{aligned} \bar{\mathbf{f}}_k &= \mathbf{\Lambda}\mathbf{f}_k + \mathbf{n} \\ &= \mathbf{\Lambda}\mathbf{D}\mathbf{s}_k + \mathbf{n} \\ &= \mathbf{\Psi}\mathbf{s}_k + \mathbf{n}, \end{aligned} \tag{12}$$

where $\mathbf{\Psi}$ is the sensing matrix. Similar to [34], we solve the non-convex combinatorial problem for the sparse vector, $\mathbf{s}_k$, given by

$$\min \|\mathbf{s}_k\|_0 \quad \text{s.t.} \quad \|\bar{\mathbf{f}}_k - \mathbf{\Psi}\mathbf{s}_k\|_2 < \sigma. \tag{13}$$

To solve the above problem, we rely on the well-known orthogonal matching pursuit (OMP) algorithm. The estimated sparse vector, $\bar{\mathbf{s}}_k$, is used to reconstruct the complete channel matrix by using $\bar{\mathbf{f}}_k = \mathbf{D}\bar{\mathbf{s}}_k$. The CE of all the incident and reflecting channels of the PU and SUs follows the same approach as explained above.

The estimated AoDs for the reflected link (i.e., from the IRS to SUs) can be utilized to sense the location of the SUs. For localization of SUs using estimated angles and path gains, we refer the readers to [35], [36].

III. Achievable Sum-rate Maximization in Second Transmission Phase

As discussed in the previous section, in the first transmission phase, the PT transmits the symbol towards the PU, which is also received by the ST. The ST helps the communication between the PT and PU by adjusting the IRS phase shifts according the PT-PU reflective channels, such that the received signal strength at the PU is maximized. Now, in the second transmission phase, the ST uses the spectrum of the primary network to serve the SUs along with the PU. For this purpose the ST employs NOMA transmission scheme. In this section, we formulate the optimization problem to maximize the weighted sum-rate of the users (both SUs and PU) in the second transmission phase. Here, we propose a method that jointly optimize the NOMA power allocation coefficients, a_k, at the ST and the phase shift matrix, $\mathbf{\Theta}^{(2)}$, of the IRS. Note that this problem is formulated for the second phase of the transmission. The achievable rate of the user in (5) and (6) can be rewritten as

$$R_k^{(2)} = \frac{1}{2} w_k \log_2 \left(1 + \frac{|\mathbf{q}_k \mathbf{u}|^2 \, a_k}{|\mathbf{q}_k \mathbf{u}|^2 \sum_{i=k+1}^{K} a_i + \sigma^2} \right) \tag{14}$$

$$R_K^{(2)} = \frac{1}{2} w_K \log_2 \left(1 + \frac{|\ \mathbf{q}_K \mathbf{u}|^2 \ a_K}{\sigma^2} \right), \tag{15}$$

where $\mathbf{q}_k = \mathbf{f}_k^H \operatorname{diag}(\mathbf{v}) \ \forall k$, $\mathbf{q}_K = \mathbf{f}_K^H \operatorname{diag}(\mathbf{v})$ and $\mathbf{u} = [e^{j\theta_1^{(2)}}, e^{j\theta_2^{(2)}}, \cdots, e^{j\theta_M^{(2)}}]^T$. After this transformation, the weighted sum-rate maximization problem can be written as

$$\text{P1:} \quad \max_{a_k, \mathbf{u}} \quad \left(\sum_{k=1}^{K-1} w_k \bar{R}_k^{(2)} \right) + w_K \bar{R}_K^{(2)} \tag{16a}$$

$$\text{s.t.} \quad |u_m| = 1, \ \forall m \tag{16b}$$

$$|\bar{\mathbf{q}}_k \mathbf{u}|^2 \geq |\bar{\mathbf{q}}_j \mathbf{u}|^2, \ \text{if } d_k < d_j \tag{16c}$$

$$a_j \geq a_k \geq 0, \ \text{if } d_j > d_k \tag{16d}$$

$$\sum_{k=1}^{K} a_k \ \leq P_{st} \tag{16e}$$

$$\bar{R}_k^{(2)} \geq r_k, \ \ k = 1, \ldots, K \tag{16f}$$

where rate values $\bar{R}_k^{(2)}$ and $\bar{R}_K^{(2)}$ denote the estimated rate using the estimated channels, such that $\bar{\mathbf{q}}_k = \bar{\mathbf{f}}_k^H \operatorname{diag}(\bar{\mathbf{v}})$. (16b) is a unit modulus constraint on the elements of $\mathbf{u}$ (i.e., IRS phase shifts) and (16c) is a user decoding order constraint. (16d) and (16e) describe the constraints on the NOMA power coefficients. Similarly, (16f) represents the rate constraint for all the users, such that r_k is the minimum rate threshold of k^{th} user.

There are two major challenges in the formulated optimization problem P1. First, the objective function is non-concave thus making the problem non-convex. Second, the NOMA power coefficients and phase shifts are coupled optimization variables making the problem more challenging.

To solve the formulated weighted sum-rate maximization optimization problem, an iterative algorithm is proposed in this paper. The variables to optimize in problem P1 are a_k (NOMA power coefficients) and $\mathbf{\Theta}^{(2)}$ (phase shift matrix). The formulated problem P1 is decomposed into two sub-problems. We show that the optimization of the phase shift matrix is required to be performed once for the problem P1. However, NOMA power coefficients are optimized in an iterative manner until convergence.

A. Optimization of Phase Shift Matrix

In the proposed algorithm, first the phase shift matrix of the IRS, $\mathbf{\Theta}^{(2)}$, is optimized by fixing the values of the NOMA power coefficients. For example, all the NOMA power coefficients can be set to the same value, such that $a_k = \frac{P_{st}}{K}$.

Then, the sub-problem for optimizing the phase shift matrix can be written as

$$\text{P1(a):} \quad \max_{\mathbf{u}} \quad \left(\sum_{k=1}^{K-1} w_k \bar{R}_k^{(2)}\right) + w_K \bar{R}_K^{(2)} \tag{17a}$$

$$\text{s.t.} \quad |u_m| = 1, \ \forall m \tag{17b}$$

$$|\bar{\mathbf{q}}_k \mathbf{u}|^2 \geq |\bar{\mathbf{q}}_j \mathbf{u}|^2, \text{ if } d_k < d_j \tag{17c}$$

In the above sub-problem P1(a), the non-convexity of the unit modulus constraint is addressed by defining a new variable, $\mathbf{V}$, where $\mathbf{V} = \mathbf{u}\mathbf{u}^H$, and $[\mathbf{V}]_{m,m} = 1$. Now, we can express (14) and (15) as

$$R_k^{(2)} = \log_2\left(1 + \text{Tr}\left(\mathbf{V}\tilde{\mathbf{Q}}_k\right) a_k\right) - \log_2\left(1 + \text{Tr}\left(\mathbf{V}\tilde{\mathbf{Q}}_k\right) a_{k+1}\right), \tag{18}$$

and

$$R_K^{(2)} = \log_2\left(1 + \text{Tr}\left(\mathbf{V}\tilde{\mathbf{Q}}_K\right) a_K\right), \tag{19}$$

respectively. Here, we define $\tilde{\mathbf{Q}}_k = \tilde{\mathbf{q}}_k^H \tilde{\mathbf{q}}_k, \forall k$, where $\tilde{\mathbf{q}}_k = \bar{\mathbf{q}}/\sqrt{\sigma^2}$. Similar to the study in [22], we introduce a new variable, $c_k = \sum_{j=k}^{K} a_j$. From this variable, the power of each user can be computed as $a_k = c_k - c_{k+1}$.

Therefore, using (18) and (19), the optimization problem P1(a) can be expressed as

$$\text{P2(a):} \quad \max_{\mathbf{V}} \quad \left(\sum_{k=1}^{K-1} w_k \left(\log_2\left(1 + \text{Tr}\left(\mathbf{V}\tilde{\mathbf{Q}}_k\right) c_k\right) - \log_2\left(1 + \text{Tr}\left(\mathbf{V}\tilde{\mathbf{Q}}_k\right) c_{k+1}\right)\right)\right) + w_K \log_2\left(1 + \text{Tr}\left(\mathbf{V}\tilde{\mathbf{Q}}_K\right) c_K\right) \tag{20a}$$

$$\text{s.t.} \quad \text{rank}\,(\mathbf{V}) = 1, \ \forall m \tag{20b}$$

$$[\mathbf{V}]_{m,m} = 1, \ \forall \ m \tag{20c}$$

$$\text{Tr}\left(\mathbf{V}\tilde{\mathbf{Q}}_k\right) \geq \text{Tr}\left(\mathbf{V}\tilde{\mathbf{Q}}_j\right), \text{ if } d_k < d_j. \tag{20d}$$

The objective function in the optimization problem P2a can be simplified by using the fact that $\text{Tr}(\mathbf{V}\tilde{\mathbf{Q}}_k) >> 1 \ \forall k$, and properties of the logarithmic function, to get

$$w_K \log_2\left(\text{Tr}\left(\mathbf{V}\tilde{\mathbf{Q}}_K\right) c_K\right) + \sum_{k=1}^{K-1} w_k \log_2\left(\frac{c_k}{c_{k+1}}\right) \tag{21}$$

It is interesting to note that the simplified objective function in (21) reveals that the IRS phase shifts are designed to benefit the K^{th} user in the studied system model. Now, we can rewrite the problem P2(a) in (20a) using (21), but the transformed optimization problem still remains non-convex due to the non-convex rank-one constraint on $\mathbf{V}$. By relaxing the rank-1 constraint and denoting $\Delta_{\mathbf{w},\mathbf{c}} = \sum_{k=1}^{K-1} w_k \log_2(c_k/c_{k+1})$, we can write the problem P2(a) as an SDR problem, given by

$$\text{P3(a):} \quad \max_{\mathbf{V}} \ w_K \log_2\left(\text{Tr}\left(\mathbf{V}\tilde{\mathbf{Q}}_K\right) c_K\right) + \Delta_{\mathbf{w},\mathbf{c}} \tag{22a}$$

$$\text{s.t.} \quad [\mathbf{V}]_{m,m} = 1, \ \forall \ m \tag{22b}$$

$$\text{Tr}\left(\mathbf{V}\tilde{\mathbf{Q}}_k\right) \geq \text{Tr}\left(\mathbf{V}\tilde{\mathbf{Q}}_j\right), \text{ if } d_k < d_j. \tag{22c}$$

After relaxing the rank-one constraint, the optimization problem P3(a) becomes an SDR problem which can be solved efficiently by a convex solver, like CVX optimization package [37], Yalimp [38] and SeDuMi. The matrix $\mathbf{V}$ obtained by solving the problem P3(a) may not be the optimal solution for the problem P2(a) as the rank of the matrix $\mathbf{V}$ can exceed the rank-one constraint. In order to get the rank-one solution, we use Gaussian randomization process [37]. In this method, the eigen decomposition of $\mathbf{V}$ is performed such that $\mathbf{V} = \mathbf{U}\mathbf{\Sigma}\mathbf{U}^H$, where $\mathbf{U}$ and $\mathbf{U}^H$ represent unitary matrices while $\mathbf{\Sigma}$ is a diagonal matrix having singular values of $\mathbf{V}$. From $\mathbf{V}$, the vector $\mathbf{u}$ containing optimal IRS phase shifts can be obtained as $\mathbf{u} = \mathbf{U}\mathbf{\Sigma}^{1/2}\mathbf{a}$, where $\mathbf{a}$ is a complex Gaussian random vector with elements having zero-mean and unit variance.

After obtaining the rank-one solution, entries of the vector $\mathbf{u}$ are transformed such that the unit modulus constraint is satisfied, such that, $\bar{\mathbf{u}}_m = \mathbf{u}_m/|\mathbf{u}_m|$ for $m = 1, \ldots, M$. The phase shift vector having the optimized values of the phase shifts is represented by $\bar{\mathbf{u}} = [e^{j\hat{\theta}_1}, e^{j\hat{\theta}_2}, \ldots, e^{j\hat{\theta}_M}]^T$ and the associated phase shift matrix for the second transmission phase is given by $\mathbf{\Theta}^{(2)} = \text{diag}(\bar{\mathbf{u}})$.

B. Optimization of NOMA Power Coefficients

Once, the phase shifts of the IRS reflecting elements are optimized for the fixed values of NOMA power coefficients, the next step is the optimization of NOMA power coefficients to maximize the weighted sum-rate of the network. As it is evident from the structure of the problem P3(a) that the optimization of IRS phase shifts is independent of the NOMA power coefficients, therefore, iterative optimization of IRS phase shifts is not required. More precisely, the optimization of IRS phase shift is only performed once at the beginning of the algorithm. On the other hand, for the optimization of the NOMA power coefficients is performed iteratively, where in each iteration the minimum rate vector $\mathbf{r} = [r_1, r_2, \ldots, r_K]$ is increased by a small positive value. Throughout the iterative process, the values of the IRS phase shifts are kept fixed as obtained in the problem P3(a). The sub-problem formulated for the optimization of NOMA power coefficients at the ST is given by

$$\text{P1(b):} \quad \max_{a_k} \quad \left(\sum_{k=1}^{K-1} w_k \bar{R}_k^{(2)}\right) + w_K \bar{R}_K^{(2)} \tag{23a}$$

$$\text{s.t.} \quad \sum_{k=1}^{K} a_k \leq P_{st} \tag{23b}$$

$$a_1 \geq \ldots, a_k \geq, \ldots, a_K \geq 0 \tag{23c}$$

$$R_k^{(2)} \geq r_k, \ \ k = 1, \ldots, K \tag{23d}$$

To solve the sub-problem P1(b) formulated in (23a), we must first determine its feasibility. According to [39], the only

condition for the feasibility of the problem P1(b) is that $P_{st} \geq \sum_{k=1}^{K} z_k$, where z_k is computed as

$$z_k = \begin{cases} \max\left\{z_{k+1}, \psi_k\left(1+\Gamma_{r,k}\sum_{j=k+1}^{K-1} z_j\right)\right\}, & k < K \\ \psi_K, & k = K \end{cases}, \tag{24}$$

where $\Gamma_k = |\bar{\mathbf{f}}_k^H \boldsymbol{\Theta}^{(2)} \bar{\mathbf{v}}|^2/\sigma^2$ is the noise normalized effective channel from the ST to k^{th} user and $\psi_k = \left(2^{(r_k)}-1\right)/\Gamma_k$. The weighted sum-rate objective function can be rewritten as

$$\sum_{k=1}^{K} w_k R_k^{(2)} = \left(\sum_{k=1}^{K-1} w_k \Big(\log_2\left(1+\Gamma_k c_k\right) - \log_2\left(1+\Gamma_k c_{k+1}\right)\Big)\right) + w_K \log_2\left(1+\Gamma_K c_K\right) \tag{25}$$

For the above objective function, the power order constraint $a_1 \geq a_2 \geq \cdots \geq a_K \geq 0$ becomes equal to $c_1 - c_2 \geq c_2 - c_3 \geq \cdots \geq c_K \geq 0$. The rate constraint $R_k \geq r_k$ can be linearized into $c_{k+1} \leq \eta_k c_k - \chi_k$ for $k = 1, \ldots, K-1$ and $c_K \geq \psi_K$ for the K^{th} user, where, $\eta_k = 2^{-r_k}$ and $\chi_k = (1-\eta_k)/\Gamma_k$ for $1, \ldots, K-1$.

Now the formulated problem P1(b) in (23a) can be rewritten using the transformed weighted sum-rate in (25), as

$$\text{P2(b):} \max_{c_1, c_2, \ldots, c_K} \left(\sum_{k=1}^{K-1} w_k \Big(\log_2\left(1+\Gamma_k c_k\right) - \log_2\left(1+\Gamma_k c_{k+1}\right)\Big)\right) + w_K \log_2\left(1+\Gamma_K c_K\right) \tag{26a}$$

$$\text{s.t.} \quad c_1 = P_{st} \tag{26b}$$

$$c_1 - c_2 \geq c_2 - c_3 \geq \cdots \geq c_K \geq \psi_K \tag{26c}$$

$$c_{k+1} \leq \eta_k c_k - \chi_k, \;\; k = 1, \ldots, K \tag{26d}$$

$$\bar{R}_k^{(2)} \geq r_k, \;\; k = 1, \ldots, K \tag{26e}$$

As the transformation between a_k and c_k variables is linear, we can conclude that if the optimization problem P1(b) in (23a) is convex then the optimization problem P2(b) in (26a) is also convex. The convexity of both the equations can be obtained from the following resulting theorem given in [39].

Theorem 1: Given that $\Gamma_1 \leq \cdots \leq \Gamma_{K-1} \leq \Gamma_K$, the weighted sum-rate optimization problems P1(a) and P1(b) are convex if any one of the following conditions is satisfied for $k = 2, \ldots, K$,

$$\text{C1}: \quad w_{k-1} \leq w_k \tag{27}$$

$$\text{C2}: \quad 1 \leq \frac{w_{k-1}}{w_k} \leq \frac{\Gamma_k^2\left(1+\Gamma_{k-1}P_{st}\right)^2}{\Gamma_{k-1}^2\left(1+\Gamma_k P_{st}\right)^2}, \tag{28}$$

When the feasibility condition is satisfied, a closed-form solution can be used to obtain the values of the variable $c_k \; \forall \; k$ using

$$c_k = \begin{cases} P_{st}, & k = 1 \\ \eta_{k-1}c_{k-1} - \chi_{k-1}, & k = 2, \ldots, K \end{cases} \tag{29}$$

Algorithm 1 Proposed algorithm for optimization of IRS phase shift and NOMA power coefficients

Inputs: P_{st}, $\mathbf{w}, \bar{\mathbf{q}}_k \; \forall \; k$, $d_k \; \forall \; k$.
Initialize: $\mathbf{a}^{(0)} = [\frac{P_{st}}{K}, \ldots, \frac{P_{st}}{K}], \mathbf{r}^{(0)} = [r_1, r_k, \ldots, r_K]$.
A. Phase shift Optimization:
1. Solve problem P3(a) in (22a) using an SDR approach and denote the obtained solution as $\mathbf{V}$.
2. Apply Gaussian randomization if the solution to problem P3(a) is not a rank-one solution to obtain $\mathbf{u}$.
3. Map the elements of $\mathbf{u}$ to $\bar{\mathbf{u}}$, such that $\bar{\mathbf{u}} = \frac{\mathbf{u}_m}{|\mathbf{u}|}$ to ensure unit-norm constraint.
4. Update $\boldsymbol{\Theta}^{(2)} = \text{diag}([\bar{\mathbf{u}}_1, \bar{\mathbf{u}}_m, \ldots, \bar{\mathbf{u}}_M]^T)$.
B. Power optimization:
1. Set the iteration number $i \leftarrow 1$
While {the problem P2(b) in (26a) is feasible}
2. Solve the problem P2(b) in (26a) using the closed form expression in (30) with fixed $\mathbf{r}^{(i)}$ and $\boldsymbol{\Theta}^{(2)}$
3. Set $i \leftarrow i+1$.
4. Set $\mathbf{r}^{(i)} \leftarrow \mathbf{r}^{(i)} + \delta$.
End While
Output: $\boldsymbol{\Theta}^{(2)}$ and $a_k \; \forall \; k$.

Then the optimal values of the NOMA power coefficients are computed, if $r_k \geq \log_2\left(2-2^{-r_{k+1}}\right)$ for $k = 1, \ldots, K-2$ and $r_{K-1} \geq 1$[2], using

$$a_k = \begin{cases} (1-\eta_k)c_k + \chi_k, & k = 1, \ldots, K-1 \\ c_K, & k = K \end{cases} \tag{30}$$

In the proposed algorithm, after obtaining the optimized NOMA power coefficients, the minimum rate threshold vector, $\mathbf{r}$, is updated by adding a small positive value δ. The feasibility of the problem P2(b) in (26a) is checked against these modified rate vector and if it is feasible then the NOMA power coefficients are calculated again. In this way, the process of computing NOMA power coefficients becomes an iterative process. On the other hand, if the problem P2(b) becomes infeasible for the given minimum rate threshold vector $\mathbf{r}$, then the algorithm stops and NOMA power coefficients computed in the previous iteration are used.

The steps involved in the proposed algorithm to solve problem P3(a) in (22a) and problem P2(b) in (26a) is summarized in Algorithm 1. In the first step of the proposed algorithm, the reflection coefficients of the IRS are optimized, while in the second step an iterative approach is used to optimize the NOMA power coefficients for all the users served by the ST.

We compare the performance of the proposed algorithm with the AO-based algorithm presented in [22] and use it as a benchmark scheme. The optimization problem P1 in (16a) in the second transmission phase is similar to the problem solved by the AO-based algorithm in [22], where the weighted sum-rate is maximized by jointly optimizing IRS phase shift matrix and NOMA power coefficients. Unlike [22], in our proposed algorithm, IRS phase shifts are optimized once at the beginning and then the values of the NOMA

[2]These two conditions can be satisfied if $r_k \geq 1$ for $k = 1, \ldots, K-1$.

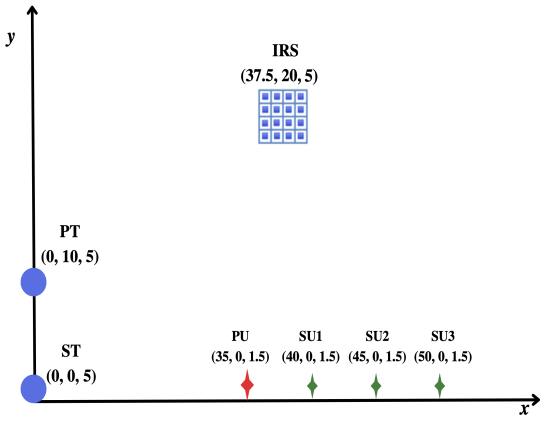

Fig. 3: Simulation setup for the considered IRS-assisted cooperative spectrum-sharing CRN with NOMA.

power coefficients are obtained iteratively until the problem P2(b) becomes infeasible for the given rate threshold vector. Therefore, our proposed scheme is computationally efficient than the AO-based algorithm presented in [22].

IV. Numerical Results

In this section, we present numerical results obtained by Monte Carlo simulations to evaluate the performance of the proposed scheme in the IRS-assisted cooperative spectrum-sharing CRN with NOMA. The performance of the proposed system is examined in terms of the overall sum-rate of the network computed as $R_p^{(1)} + \sum_k^K w_k R_k^{(2)}$ and SUs sum-rate given by $\sum_k^{K-1} w_k R_k^{(2)}$. In the simulation setup, we consider a two-dimensional coordinate system as shown in Fig. 3, where the PT is located at (0,10,5) meters (m) and the ST is placed at (0,0,5)m.

The users (i.e., PU and SUs) are located on the horizontal axis in the range of 30m to 50m from the ST. In addition, a single IRS is deployed at point (37.5,20,5)m, having a total of M number of reflective elements arranged in a uniform planar array fashion. The inter-element space is set to a half wavelength i.e. $d_{\text{IRS}} = \lambda/2$. Throughout this section, we set $M_v = 5$ and $M_h = M/M_h$. Similar to [22], in this study, the large-scale path loss between the i^{th} and the j^{th} nodes in the network is modeled as

$$PL_{i,j} = \frac{C_0}{(d_{i,j})^{\epsilon}} \tag{31}$$

where $C_0 = -30$ dB is the path loss at a reference distance of 1 m, $d_{i,j}$ is the distance of the (i,j) link. Similarly, $\epsilon = 2.2$ is the path loss exponent of the incident channels and $\epsilon = 2.4$ denotes the path loss exponent of the reflected channels [40]. We assume $\mathbf{w}_k = 1\ \forall k$ as the weight vector and $\mathbf{r}^{(0)} = [1,1,1,1]$ bps/Hz, representing the unweighted minimum rate requirements for both PU and SUs. The noise power at the users is set to $\sigma^2 = -110$ dBm [41]. Unless otherwise stated, the same parameters are used throughout the simulation. The results presented in this section are averaged over large number of channel realizations.

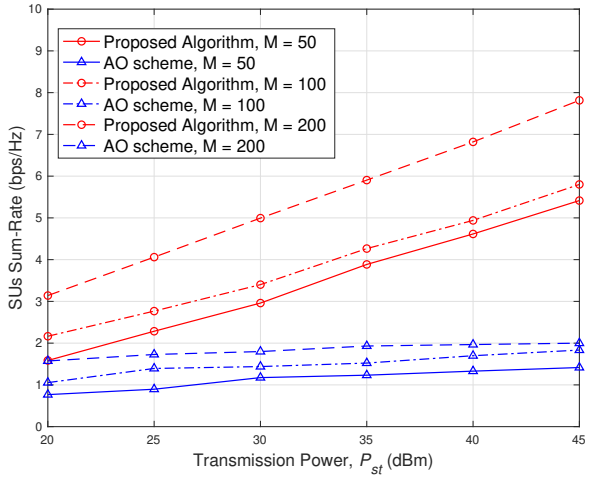

Fig. 4: Sum-rate results against the range of transmission power values.

A. SUs sum-rate

In Fig. 4, the performance of the proposed technique is shown with regards to the SUs sum-rate. With $K = 4$ users, the SUs sum-rate corresponds to the rate of the first $K-1$ users, i.e., excluding the PU rate. In particular, we plot the sum-rate against different values of the transmission power, P_{st}. Here, results with different values of the total number of reflective elements in the IRS, i.e., $M = \{50, 100, 200\}$ are plotted. To demonstrate the effectiveness of the proposed IRS phase shift optimization and NOMA power allocation technique, it is compared with AO-based algorithm [22]. It is evident from Fig. 4 that the proposed optimization technique outperforms the AO-based scheme. The reason for the improved performance is due to the fact that AO-based scheme in [22] uses first order Taylor expansion to transform the non-convex problem P1(a) to a convex problem. On the contrary, we transformed the non-convex optimization problem to a convex problem using properties of the logarithmic function to simplify the problem which then results in a convex SDR problem. The optimization of NOMA power coefficients presented in this study assigns more power to the users with low SNRs. Moreover, Fig. 4 also indicates that the performance of both the schemes improves as the number of IRS elements are increased.

In Fig. 5, the SUs sum-rate is plotted against the total number of reflective elements in the IRS, M. Here, we set $K = 4$ and $P_{st} = 40$ dBm. It is observed that as M increases, the sum-rate exhibits a ceiling effect. This trend is evident in both the schemes. This means that having an IRS with a large number of reflective elements may not improve the sum-rate performance of the secondary network but it will in fact increase the computational complexity of the system. This trend indicates that the deployed IRS should have optimal number of reflective elements such that a sum-rate performance improvement is achieved without enhancing the complexity of the system.

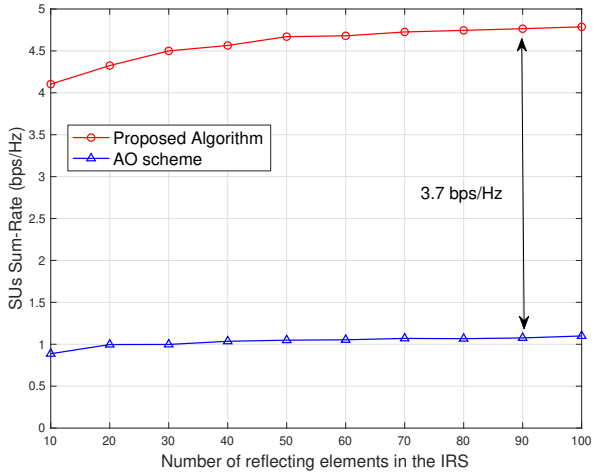

Fig. 5: Sum-rate performance against the different values of the total number of reflecting elements, M.

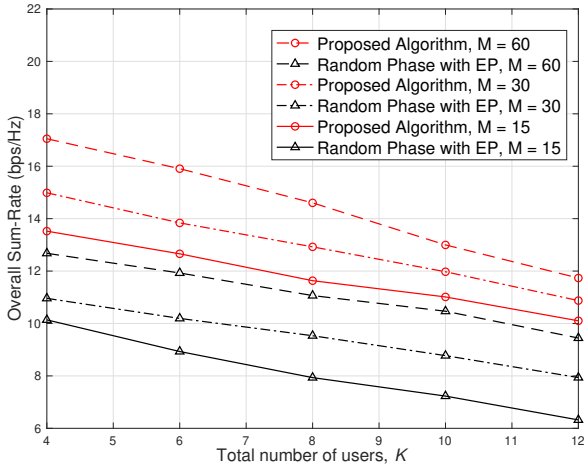

Fig. 7: Sum-rate performance versus the total number of users in the network with $P = 40$ dBm.

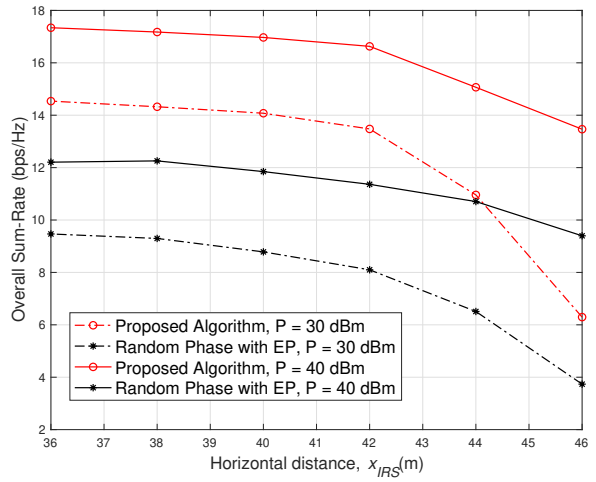

Fig. 6: Sum-rate performance by varying the location of IRS with $M = 64$ and $K = 4$.

B. Overall sum-rate

In order to investigate the effect of the IRS location on the performance of the system, in Fig. 6, we plot the overall sum-rate performance of the network by varying the location of the IRS. Here, we compare the performance of the proposed scheme with the random phase shift scheme. In the random phase shift scheme, the reflection coefficients of the IRS are set randomly within the interval $[0, 2\pi)$ and equal power (EP) allocation at the ST. The first transmission phase (discussed in Section II-A) is same for both the schemes, i.e., both the schemes plotted in Fig. 6 have equal PU rate during the first transmission phase. We set equal transmission power values for the PT and ST, such that $P = P_p = P_{st}$. For these results, we consider $M = 60$, $K = 4$, and $P = \{30, 40\}$ dBm, while the coordinates of the IRS are set as $(x_{\text{IRS}}, 20, 5)$, where $x_{\text{IRS}} = \{36, 38, 40, 42, 44, 46\}$. Note that by increasing the value of x_{IRS}, the IRS moves away from the ST. The trend in Fig. 6 depicts that the overall sum-rate of the network is higher when the IRS is deployed near to the ST.

Figure 7 shows the overall sum-rate results of the network against the total number users in the network, K. We fix the transmission power of the PT and ST at $P = 40$ dBm and the number of reflective elements varies from 15 to 60. It is evident from the figure that the proposed algorithm outperforms the random phase shift scheme with EP. For the reversal of the downward trend, both transmission power and the number of IRS reflecting elements can be increased when the number of users (i.e., PU and SUs) increases in the network.

V. CONCLUSION

In this paper, we have investigated an IRS-assisted cooperative spectrum-sharing CRN with NOMA. The rationale behind the cooperative spectrum-sharing CRN is that the secondary network uses the spectrum assigned to the primary network. In return, the secondary network re-transmits the primary network messages while using the NOMA scheme. This approach to sharing spectrum resources facilitates the network's capacity to cater to a larger number of users within the available spectrum. The proposed transmission strategy comprises of two sequential stages, with the second stage tailored towards optimizing the network's weighted sum-rate. This optimization involves fine-tuning IRS phase shifts and the NOMA power coefficients at the ST. To effectively manage the non-convexity of the weighted sum-rate problem, a bifurcation into two sub-problems is executed. These sub-problems are solved through a computationally efficient algorithm. We employ semi-passive IRS which with the help of active and passive IRS elements is capable of performing simultaneous downlink data transmission for the primary network and CE for the secondary network during the first transmission phase.

In the presented algorithm, the optimization of IRS phase shifts is executed once at the beginning by employing the SDR methodology. Following this, the optimization of NOMA

power coefficients at the ST is undertaken in an iterative fashion. The performance of the proposed algorithm is illustrated via simulations, demonstrating its superiority when compared to the benchmark AO-based optimization strategy. The optimization framework used in this paper can be extended to the scenario where users are assisted by multiple IRSs. The optimal assignment of IRSs to the users is an interesting topic for future work.

REFERENCES

[1] Y. Zeng and R. Zhang, "Millimeter wave MIMO with lens antenna array: A new path division multiplexing paradigm," *IEEE Transactions on Communications*, vol. 64, no. 4, pp. 1557–1571, Apr. 2016.

[2] F. Tariq, M. R. Khandaker, K.-K. Wong, M. A. Imran, M. Bennis, and M. Debbah, "A speculative study on 6G," *IEEE Wireless Communications*, vol. 27, no. 4, pp. 118–125, Aug. 2020.

[3] H. Tataria, M. Shafi, A. F. Molisch, M. Dohler, H. Sjöland, and F. Tufvesson, "6G wireless systems: Vision, requirements, challenges, insights, and opportunities," *Proceedings of the IEEE*, vol. 109, no. 7, pp. 1166–1199, Jul. 2021.

[4] W. Jiang, B. Han, M. A. Habibi, and H. D. Schotten, "The road towards 6G: A comprehensive survey," *IEEE Open Journal of the Communications Society*, vol. 2, pp. 334–366, Feb. 2021.

[5] Y. Yuan, Y. Zhao, B. Zong, and S. Parolari, "Potential key technologies for 6G mobile communications," *Science China Information Sciences*, vol. 63, no. 8, pp. 1–19, Nov. 2020.

[6] E. Basar, M. Di Renzo, J. De Rosny, M. Debbah, M.-S. Alouini, and R. Zhang, "Wireless communications through reconfigurable intelligent surfaces," *IEEE access*, vol. 7, pp. 116 753–116 773, Jun. 2019.

[7] Q. Wu, S. Zhang, B. Zheng, C. You, and R. Zhang, "Intelligent reflecting surface-aided wireless communications: A tutorial," *IEEE Transactions on Communications*, vol. 69, no. 5, pp. 3313–3351, May 2021.

[8] Q. Wu and R. Zhang, "Towards smart and reconfigurable environment: Intelligent reflecting surface aided wireless network," *IEEE Communications Magazine*, vol. 58, no. 1, pp. 106–112, Nov. 2019.

[9] K. Feng, X. Li, Y. Han, S. Jin, and Y. Chen, "Physical layer security enhancement exploiting intelligent reflecting surface," *IEEE Communications Letters*, vol. 25, no. 3, pp. 734–738, Mar. 2021.

[10] S. Gong, Z. Yang, C. Xing, J. An, and L. Hanzo, "Beamforming optimization for intelligent reflecting surface-aided SWIPT IoT networks relying on discrete phase shifts," *IEEE Internet of Things Journal*, vol. 8, no. 10, pp. 8585–8602, May 2020.

[11] A. Puglielli, N. Narevsky, P. Lu, T. Courtade, G. Wright, B. Nikolic, and E. Alon, "A scalable massive MIMO array architecture based on common modules," in *proc. IEEE International Conference on Communication Workshop (ICCW)*, London, UK, 2015, pp. 1310–1315.

[12] S. Hu, F. Rusek, and O. Edfors, "Beyond massive MIMO: The potential of data transmission with large intelligent surfaces," *IEEE Transactions on Signal Processing*, vol. 66, no. 10, pp. 2746–2758, May 2018.

[13] J. Zhu, Y. Huang, J. Wang, K. Navaie, W. Huang, and Z. Ding, "On the position optimization of IRS," *IEEE Internet of Things Journal*, vol. 9, no. 14, pp. 11 712–11 724, Jul. 2022.

[14] Q. Wu and R. Zhang, "Intelligent reflecting surface enhanced wireless network via joint active and passive beamforming," *IEEE Transactions on Wireless Communications*, vol. 18, no. 11, pp. 5394–5409, Nov. 2019.

[15] C. Huang, A. Zappone, G. C. Alexandropoulos, M. Debbah, and C. Yuen, "Reconfigurable intelligent surfaces for energy efficiency in wireless communication," *IEEE Transactions on Wireless Communications*, vol. 18, no. 8, pp. 4157–4170, Nov. 2019.

[16] X. Yu, D. Xu, and R. Schober, "MISO wireless communication systems via intelligent reflecting surfaces," in *proc. IEEE/CIC International Conference on Communications in China (ICCC)*, Changchun, China, 2019, pp. 735–740.

[17] P. Wang, J. Fang, X. Yuan, Z. Chen, and H. Li, "Intelligent reflecting surface-assisted millimeter wave communications: Joint active and passive precoding design," *IEEE Transactions on Vehicular Technology*, vol. 69, no. 12, pp. 14 960–14 973, Dec. 2020.

[18] H. Wang, C. Liu, Z. Shi, Y. Fu, and R. Song, "On power minimization for IRS-aided downlink NOMA systems," *IEEE wireless communications letters*, vol. 9, no. 11, pp. 1808–1811, Nov. 2020.

[19] M. Fu, Y. Zhou, and Y. Shi, "Intelligent reflecting surface for downlink non-orthogonal multiple access networks," in *proc. IEEE Globecom Workshops*, Waikoloa, HI, USA, 2019, pp. 1–6.

[20] Z. Ding and H. V. Poor, "A simple design of IRS-NOMA transmission," *IEEE Communications Letters*, vol. 24, no. 5, pp. 1119–1123, May 2020.

[21] G. Yang, X. Xu, and Y.-C. Liang, "Intelligent reflecting surface assisted non-orthogonal multiple access," in *proc. IEEE wireless communications and networking conference (WCNC)*, Seoul, South Korea, 2020, pp. 1–6.

[22] X. Mu, Y. Liu, L. Guo, J. Lin, and R. Schober, "Joint deployment and multiple access design for intelligent reflecting surface assisted networks," *IEEE Transactions on Wireless Communications*, vol. 20, no. 10, pp. 6648–6664, Oct. 2021.

[23] J. Yuan, Y.-C. Liang, J. Joung, G. Feng, and E. G. Larsson, "Intelligent reflecting surface (IRS)-enhanced cognitive radio system," in *proc. IEEE International Conference on Communications (ICC)*, Dublin, Ireland, 2020, pp. 1–6.

[24] J. Yuan, Y.-C. Liang, J. Joung, G. Feng, and Larsson, "Intelligent reflecting surface-assisted cognitive radio system," *IEEE Transactions on Communications*, vol. 69, no. 1, pp. 675–687, Jan. 2020.

[25] D. Xu, X. Yu, and R. Schober, "Resource allocation for intelligent reflecting surface-assisted cognitive radio networks," in *proc. IEEE 21st International Workshop on Signal Processing Advances in Wireless Communications (SPAWC)*, Atlanta, Georgia, USA, 2020, pp. 1–5.

[26] Y. Wu, F. Zhou, W. Wu, Q. Wu, R. Q. Hu, and K.-K. Wong, "Multi-objective optimization for spectrum and energy efficiency tradeoff in IRS-assisted CRNs with NOMA," *IEEE Transactions on Wireless Communications*, vol. 21, no. 8, pp. 6627–6642, Aug. 2022.

[27] T.-T. T. Nguyen, X.-X. Nguyen, and H. H. Kha, "Secrecy outage performance analysis for IRS-aided cognitive radio NOMA networks," in *proc. IEEE Ninth International Conference on Communications and Electronics (ICCE)*, Nha Trang City, Vietnam, 2022, pp. 149–154.

[28] W. Liang, W. Luo, J. Zhang, and Z. Ding, "Active and passive beamforming design for reconfigurable intelligent surface assisted CR-NOMA networks," *IEEE Communications Letters*, vol. 26, no. 10, pp. 2409–2414, Oct. 2022.

[29] R. Alhamad, "NOMA using intelligent reflecting surfaces with adaptive transmit power and multi-antennas energy harvesting," *Wireless Networks*, vol. 28, no. 3, pp. 1–10, Apr. 2022.

[30] L. Lv, Q. Ni, Z. Ding, and J. Chen, "Application of non-orthogonal multiple access in cooperative spectrum-sharing networks over nakagami-m fading channels," *IEEE Transactions on Vehicular Technology*, vol. 66, no. 6, pp. 5506–5511, Jan. 2016.

[31] Y.-C. Liang, R. Long, Q. Zhang, J. Chen, H. V. Cheng, and H. Guo, "Large intelligent surface/antennas (LISA): Making reflective radios smart," *Journal of Communications and Information Networks*, vol. 4, no. 2, pp. 40–50, Jun. 2019.

[32] R. W. Heath, N. González-Prelcic, S. Rangan, W. Roh, and A. M. Sayeed, "An overview of signal processing techniques for millimeter wave MIMO systems," *IEEE Journal of Selected Topics in Signal Processing*, vol. 10, no. 3, pp. 436–453, 2016.

[33] Y. Heng and J. G. Andrews, "Grid-less mmWave beam alignment through deep learning," in *Proc. IEEE Global Communications Conference*, Rio de Janeiro, Brazi, 2022, pp. 2290–2295.

[34] A. Taha, M. Alrabeiah, and A. Alkhateeb, "Enabling large intelligent surfaces with compressive sensing and deep learning," *IEEE Access*, vol. 9, pp. 44 304–44 321, 2021.

[35] X. Hu, C. Liu, M. Peng, and C. Zhong, "IRS-based integrated location sensing and communication for mmWave SIMO systems," *IEEE Transactions on Wireless Communications*, vol. 22, no. 6, pp. 4132–4145, 2023.

[36] Z. Yu, X. Hu, C. Liu, M. Peng, and C. Zhong, "Location sensing and beamforming design for IRS-enabled multi-user ISAC systems," *IEEE Transactions on Signal Processing*, vol. 70, pp. 5178–5193, 2022.

[37] N. Sidiropoulos, T. Davidson, and Z.-Q. Luo, "Transmit beamforming for physical-layer multicasting," *IEEE Transactions on Signal Processing*, vol. 54, no. 6, pp. 2239–2251, Jun. 2006.

[38] J. Lofberg, "Yalmip: A toolbox for modeling and optimization in matlab," in *proc. IEEE international conference on robotics and automation*, Taipei, Taiwan, 2004, pp. 284–289.

[39] J. Wang, Q. Peng, Y. Huang, H.-M. Wang, and X. You, "Convexity of weighted sum rate maximization in NOMA systems," *IEEE signal processing letters*, vol. 24, no. 9, pp. 1323–1327, Sep. 2017.

[40] C. Pan, H. Ren, K. Wang, M. Elkashlan, A. Nallanathan, J. Wang, and L. Hanzo, "Intelligent reflecting surface aided MIMO broadcasting for simultaneous wireless information and power transfer," *IEEE Journal on Selected Areas in Communications*, vol. 38, no. 8, pp. 1719–1734, Aug. 2020.

[41] G. Tian and R. Song, "Cooperative beamforming for a double-IRS-assisted wireless communication system," *EURASIP Journal on Advances in Signal Processing*, vol. 2021, pp. 1–10, Aug. 2021.